

FLORIDA INTERNATIONAL UNIVERSITY

Miami, Florida

UNDERSTANDING THE CORRELATION BETWEEN ELASTIN  
ABUNDANCE, MELANOCYTIC EXPRESSION, AND THE PRESENCE OF  
PIGMENTATION WITHIN THE AORTIC VALVE IN A MOUSE MODEL

A thesis submitted in partial fulfillment of the

requirements for the degree of

MASTER OF SCIENCE

in

BIOMEDICAL ENGINEERING

by

Aasma Dahal

2023

To: Dean John L. Volakis  
College of Engineering and Computing

This dissertation, written by Aasma Dahal, and entitled Understanding the Correlation between Elastin Abundance, Melanocytic Expression and the Presence of Pigmentation within the Aortic Valve in a Mouse Model, having been approved in respect to style and intellectual content, is referred to you for judgment.

We have read this dissertation and recommend that it be approved.

---

Lidia Kos

---

Sharan Ramaswamy

---

Joshua Hutcheson, Major Professor

Date of Defense: June 7, 2023

The dissertation of Aasma Dahal is approved.

---

Dean John L. Volakis  
College of Engineering and Computing

---

Andres Gil  
Vice President for Research and Economic Development  
and Dean of the University Graduate School

Florida International University, 2023

## DEDICATION

I would like to dedicate this work to my parents, whose love and support have been instrumental in shaping who I am today. To my mother, thank you for your unwavering belief in me and for always pushing me to be my best self. To my father, thank you for your wisdom, guidance, and encouragement, and for instilling in me a passion for learning and growth. I am truly blessed to have such amazing parents and sisters, and I cannot express enough how grateful I am for everything you have done for me. This work reflects the values and lessons you have imparted upon me, and it is with great pride and gratitude that I dedicate it to you.

## ACKNOWLEDGMENTS

I would like to take this opportunity to express my sincere gratitude to all those who have supported me throughout my thesis work. Without their unwavering support, encouragement, and guidance, I would not have been able to reach this point in my academic journey. First and foremost, I want to dedicate this work to everyone who has been a constant source of support for me. My family and friends have been my backbone, cheering me up when I felt low and motivating me to push through challenges. Their unwavering support and encouragement have been invaluable to me, and I could not have done this without them. I love you all. I would also like to extend my heartfelt thanks to Fulbright Nepal for providing me with financial support and making this research possible. I am grateful to the University Graduate School at FIU for their professional support, which has been crucial to the success of my research.

I am deeply grateful to my exceptional supervisor, Dr. Hutcheson, for his constant support, encouragement, and guidance. His mentorship has been instrumental in shaping my scientific thinking and approach, and I cannot thank him enough for his unwavering dedication to my success. Dr. Hutcheson's patience and understanding, even during the times when I may have fallen short, have not gone unnoticed and have made a significant impact on my personal and professional growth. I consider myself privileged to work under his leadership, and I look forward to continuing to learn and grow under his expert guidance. His invaluable mentorship has not only shaped my career but has also made a profound impact on my personal and professional life. Thanks for keeping your door open for me always and inspiring me to strive for excellence every day.

I also want to express my gratitude to Dr Kos for her support and assistance. Her expertise and knowledge have been vital, and I am fortunate to have had an

opportunity to work with her. Dr Kos, you are an amazing human who adds color to light up the environment. Her contributions to my research are greatly appreciated. In addition, I would like to extend my sincere appreciation to Dr. Ramaswamy for his support throughout my research. His insights and guidance have been crucial to my academic success. I appreciate his dedication to students and his commitment to helping us achieve our academic goals.

I want to acknowledge my mentor, Daniel Chaparro, for his invaluable guidance and support throughout my academic and personal journey. Daniel has been much more than a mentor to me - he has been a trusted friend and go-to person, who has always been there to lend an ear or offer valuable advice. His wise guidance has been instrumental in shaping my academic pursuits and personal growth. I deeply appreciate his patience, understanding, and encouragement during the times when I needed it the most. His mentorship has made a profound impact on my academic success and personal life. I feel truly fortunate to have him in my life, and I thank him sincerely for being an exceptional mentor and friend.

I would like to express my deep appreciation to Mary for her unwavering support and kindness during my stay in Miami. The memories of my time here will always hold a special place in my heart, and I will never forget the warmth and hospitality that Mary extended to me. I also want to give a special thanks to my dear friends, Pratik, Seema-Neha Sunil-Arju, Abhishek-Anshu, Sudip-Suraksha, Veeru, and my friends from South Florida Fulbright Chapter, for being a family to me and for their constant support and friendship. Your presence in my life has meant everything to me. Additionally, I am grateful to Mohammad Shaver, Perony Nogueira, Denise Hsu, and Valentina Dargam for their guidance and assistance. Thank you, Daniela, and Julio, for making work in the cubicle much more enjoyable with your positive attitudes, friendly personalities, and willingness to help. Finally, I want to

thank the entire CMRL crew for making lab enjoyable and fun. Working with such amazing colleagues/friends has been a privilege, and I appreciate your outstanding contributions.

Thank you all once again for your support, encouragement, and guidance throughout my thesis work. Your contributions have been invaluable, and I am fortunate to have had the opportunity to work with such amazing people.

ABSTRACT OF THE THESIS  
UNDERSTANDING THE CORRELATION BETWEEN ELASTIN  
ABUNDANCE, MELANOCYTIC EXPRESSION, AND THE PRESENCE OF  
PIGMENTATION WITHIN THE AORTIC VALVE IN A MOUSE MODEL

by

Aasma Dahal

Florida International University, 2023

Miami, Florida

Professor Joshua Hutcheson, Major Professor

The aortic valve is a complex structure responsible for blood flow from left ventricle to aorta. The elasticity and function of the valve is largely dependent on the presence of elastic fibers. Previous studies report a correlation between Aortic Valve (AoV) Leaflets melanocytic pigmentation and elastic fiber abundance. However, the involvement of melanocytes in elastogenesis is unknown. In this study, we aimed to investigate the correlation between the presence of melanocytic pigments, melanocytic gene expression, and elastic fiber abundance in the AoV leaflets. To achieve this, we utilized three mouse models with different pigmentation. We performed fluorescence staining to visualize the elastic fibers abundance and analyzed the expression of melanocytic markers (Tyr and DCT) using RT-qPCR. Our results suggest that neither the presence/absence of melanocytic markers or pigments alone is sufficient to explain the observed elastin phenotype and additional mechanisms likely contribute to elastogenesis beyond pigmentation or melanocytic gene expression.

## TABLE OF CONTENTS

CHAPTER	PAGE
1. INTRODUCTION . . . . .	1
1.1 Structure of the human heart . . . . .	1
1.1.1 Aortic Valve . . . . .	1
1.1.2 Aortic Valve structure . . . . .	2
1.1.3 Research questions . . . . .	9
2. METHODOLOGY . . . . .	10
2.1 Animals used . . . . .	10
2.2 Fluorescence Staining/Elastin-Collagen Assay . . . . .	10
2.2.1 Procedure . . . . .	11
2.2.2 Imaging . . . . .	12
2.2.3 Image Quantification . . . . .	12
2.3 RT-qPCR Reverse Transcription quantitative Polymerase Chain reaction	14
3. RESULTS . . . . .	16
3.1 <u>Pigmentation in WT1, WT2, Albino, KH:</u> . . . . .	16
3.2 <u>Elastin Abundance in WT1, WT2, Albino and KH:</u> . . . . .	16
3.3 <u>Melanocytic expression in WT1, WT2, Albino and KH:</u> . . . . .	19
4. DISCUSSION . . . . .	20
5. CONCLUSION . . . . .	24
REFERENCES . . . . .	25

## LIST OF FIGURES

FIGURE	PAGE
1.1	Structure of heart showing all the valves and the Schematic diagram of the leaflets-Left Coronary Cusp(LCC),Right Coronary Cusp(RCC) and Non Coronary Cusp(NCC)(Illustration created with Bio-Render.com) 2
1.2	A) The mature aortic valve contains fibrosa facing aorta, ventricularis facing the left ventricle, and spongiosa, middle of the two layers. B)Cellular architecture of the aortic valve- the valvular endothelial cells(VECs) lies on the outer both sides of the valve with the three layers of the valve in between the VECs-fibrosa, spongiosa, and ventricularis,consisting of VICs as the predominant cell type. The fibrosa contains more Type I and Type III fibrillar collagen. The spongiosa comprises of glycosaminoglycans (GAGs) and the ventricularis contains more elastic fibers.(Illustrations created using Biorender.com) 4
1.3	Figure showing the pigments in the leaflets of C57BL/6J (WT)mouse . . 8
2.1	The figure illustrates the elastic(in red) and collagen(in green) fibers present in the leaflets of the AoV. Customized code and threshold are utilized to determine the area of each leaflet (Fig. B, E, H). Additionally, the MFI of AF633 is employed to measure the elastin abundance within the leaflets (Fig. C, F, I). . . . . 13
2.2	Table 1: Primer DCT, TYR, GAPDH along with their sequences. . . . 15
3.1	The aortic valve structure showing the melanocytic pigments and different section in the valve apparatus. In 56% of WT mice, all LCC, RCC and NCC are pigmented. B) In 44% of the WT mice, the LCC doesn't have melanocytic pigments whereas the RCC and NCC are pigmented. C) and D) The Albino and the KitHet mice (respectively) doesn't have pigment in any of the cusps. . . . . 17
3.2	Elastin based elastic fibre alignment in AoV leaflets-In murine AoV leaflets, these elastic fibers on the ventricularis surface of the valve cusp are aligned radially A), and they transition to a circumferential orientation as they approach the fibrosa B) . . . . . 17
3.3	Elastic fibers abundance in the AoV leaflets in different mouse models. Fig 3.3A shows the fiber abundance in WT1, WT2, Albino and KH mice normalized to the area of the respective leaflets. Fig 3.3B,3.3C, 3.3D, 3.3E shows the varying amount of elastic fiber in LCC, RCC, NCC of AoV leaflets in these classified four groups, WT1, WT2, Albino, and KH respectively.) . . . . . 18
3.4	Expression of DCT within the AoV leaflets in different mouse models showing significant difference between the WT2 and the rest of mouse models. However, it does not show any significant difference between the WT1, Albino and KH. . . . . 19

4.1 Different levels of pigmentation seen in the leaflets. The LCC of (A) has more pigments than the LCC in fig. (C) (shown by red arrow). The cause of this different level of pigmentation is still unclear and requires more detailed cellular study. . . . . 20

## ABBREVIATIONS AND ACRONYMS

AF633	Alexa Flour 633
ANOVA	Analysis of Variance
AoV	Aortic Valve
DCT	Dopachrome Tautomerase
ECM	Extracellular Matrix
Eln	Elastin
GAG	Glycosaminoglycan
KH	Kit Heterozygous
LCC	Left-Coronary Cusp
MIP	Mean Fluorescence Intensities
NCC	Non-Coronary Cusp
PBS	Phosphate Buffered Saline
PFA	Paraformaldehyde
RCC	Right-Coronary Cusp
RT-qPCR	Reverse Transcription quantitative Polymerase Chain Reaction
TYR	Tyrosinase
VECs	Valvular Endothelial Cells
VICs	Valvular Interstitial Cells
WT	Wild Type
$\delta$ Ct	Cycle threshold
$\mu$ m	micron

# CHAPTER 1

## INTRODUCTION

### 1.1 Structure of the human heart

The human heart is a muscular organ in the chest that circulates blood throughout the body. A complex network of arteries, veins, and capillaries carries blood to and from the rest of the body. Valves within the heart help maintain unidirectional blood flow throughout the cardiac cycle. These four valves, tricuspid, pulmonary, aortic, and mitral valves, help regulate blood flow through the heart and prevent backward flow. The aortic valve, located between the left ventricle and the aorta, opens during systole to allow blood flow from the left ventricle into the aorta and closes to prevent blood from flowing backward into the left ventricle during diastole. The heart valves open and close in response to changes in pressure within the heart chambers. They are essential for maintaining blood flow through the heart and ensuring it is pumped efficiently to the rest of the body.

#### 1.1.1 Aortic Valve

The aortic valve has three leaflets, or cusps, which open and close to control blood flow from the left ventricle to the aorta, ensuring the blood flows in one direction, from the heart to the rest of the body. These cusps can withstand extreme mechanical and hemodynamic forces due to their complex geometry and cellular composition. Any changes in these components may hamper the overall function of the valve. For example, bicuspid valve malformations—where an individual has two aortic valve cusps rather than three—is a major cause of calcific aortic valve disease. The cusps encounter a variety of stresses during the cardiac cycle, such

as shear stress, leaflet strain in both radial and circumferential directions, pressure exerted on the cusp surface during diastole, and bending force during valve closure. The ventricular side of the cusps encounters high blood velocity and shear stress during valve opening, while the aortic side is subjected to complex, oscillatory flow during closure. The responses to this diverse mechanical stress are regulated by valve cellular and extracellular matrix components. Figures 1.1(a), 1.1(b) show the blood flow in the heart and the cellular architecture of the aortic valve within the heart.

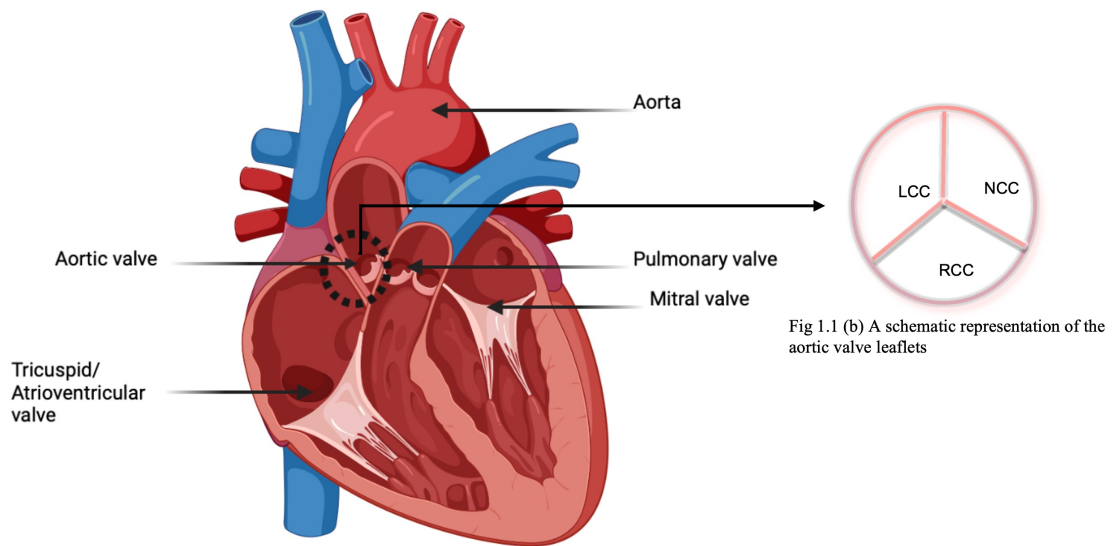


Fig 1.1 (a) Structure of heart showing all the valves

Fig 1.1 (b) A schematic representation of the aortic valve leaflets

Figure 1.1: Structure of heart showing all the valves and the Schematic diagram of the leaflets-Left Coronary Cusp(LCC),Right Coronary Cusp(RCC) and Non Coronary Cusp(NCC)(Illustration created with Bio-Render.com)

### 1.1.2 Aortic Valve structure

The aortic valve is primarily composed of two cell types—valve endothelial cells and valve interstitial cells—that maintain the extracellular matrix structure. The

valve endothelial cells cover the outer portion of the cusps, where they interface with the blood flowing out of the heart, and the valve interstitial cells reside within the trilaminar valvular structure with well-defined layers enriched in collagen, glycosaminoglycans, and elastic fibers (Carruthers et al. 2012). The orientation and function of this unique structure is described in more detail in the following sections.

#### **1.1.2.1 Valvular cellular components**

The Aortic Valve (AoV) consists of a layer of connective tissue- VECs, lined together in the adjacent sides of the aorta (ventricularis and fibrosa) as shown in figure(1.1.2.1). These cells interact with blood and associated hemodynamic forces to protect the valve from damage and keep it smooth and functional. Fibrosa-side VECs are phenotypically different from the ventricularis VECs (Bischoff and Aikawa, 2011). The abnormal hemodynamic forces in the cusps cause tissue remodeling and inflammation leading to stenosis, sclerosis, calcification, and valve failure. Studies have shown that VECs play an important role in maintaining valvular development during the embryonic stage and valvular integrity throughout (Lincoln and Yutzey, 2011).

Similarly, VICs are another abundant cellular layer in the Aortic cusps, comprising of  $\alpha$ -actin( $\alpha$ SMA), fibroblasts, myofibroblasts, neurons and glia, which aid in valvular contraction and the synthesis of extracellular matrix components, enabling constant remodeling within the cusps. VICs also play a crucial role in normal development, function, and homeostasis in ECM (Rajamannan et al., 2011). VICs interact with VECs to maintain the ECM integrity and intervene in diseases. These cells respond to physical stress and the biological protein/molecules present in the blood which helps to regulate the components of the extracellular matrix, the tension within the valve, and the renewal of the cell population. Studies have shown that

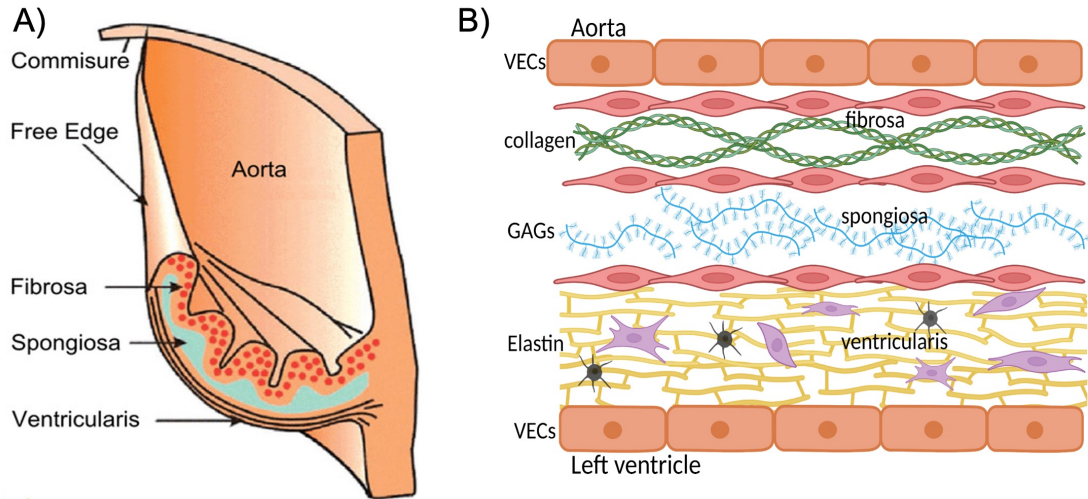


Figure 1.2: A) The mature aortic valve contains fibrosa facing aorta, ventricularis facing the left ventricle, and spongiosa, middle of the two layers. B) Cellular architecture of the aortic valve- the valvular endothelial cells(VECs) lies on the outer both sides of the valve with the three layers of the valve in between the VECs-fibrosa, spongiosa, and ventricularis,consisting of VICs as the predominant cell type. The fibrosa contains more Type I and Type III fibrillar collagen. The spongiosa comprises of glycosaminoglycans (GAGs) and the ventricularis contains more elastic fibers.(Illustrations created using Biorender.com)

mechanical stress in valve can increase the secretion of matrix remodeling enzymes, and growth factors in the Aortic valve (Ku et al., 2006).Alongside the VICs and VECs, there are a group of melanocyte-positive cells normally distributed in the tri-cuspid and mitral valvular leaflets of a typical mouse heart (C57BL/6) (Mjaatvedt et al., 2005) however the direct role of melanocytic cells in the ECM remodeling in the aortic valve is still unknown.

### 1.1.2.2 Extracellular Matrix (ECM)

On the aortic aspect of the aortic valve, within the fibrosa, the cusps have a dense circumferentially aligned collagenous layer consisting of collagen types I and III, which provide tensile strength during the valve closure (Rajamannan et al., 2011).

Below the fibrosa is a layer known as the spongiosa, which is rich in glycosaminoglycans (GAGs). This layer helps absorb compressive forces and aids in the interactions between the highly structured elastic and collagen fibers. The elastin-rich ventricularis, below the spongiosa on the ventricular aspect of the valve, supports the tissue load at low strains, allowing the collagen fibers and the cusp to passively stretch to support changes in load. These elastic fibers are radially aligned on the ventricularis surface of the valve cusp and become circumferentially aligned towards the fibrosa in the murine valve (Nasim et al., 2021). This orientation in the valve allows the cusps to stretch and seal the valve during the closure and spring open to provide minimal resistance to blood flow. Alteration in these structural and functional changes of elastin leads to disease, and ultimately, valve failure (Cocciolone et al., 2018).

With aging and due to other factors, such as genetics or inflammation, the degradation and fragmentation of elastin fibers occur, causing the valve to lose its elasticity. This can result in valve disease, eventually leading to valve failure (Green et al., 2014)). Many studies have focused on the role of collagen in valve development and disease. The factors regulating elastic fiber formation remain unclear. Here, we seek to better characterize regional heterogeneity in elastin patterning and phenotypes associated with altered elastogenesis.

## **Elastic Fibers**

The elastic fibers in the Aortic valve have a vital role in conferring elasticity, aiding the opening, and closing of the valve. Radially aligned elastin-rich fibers originate from the ventricularis and become circumferentially aligned towards the fibrosa (Biliar and Sacks 1999; Latif et al., 2005). This alignment is essential in valve closure during diastole and to restore its original shape and orientation during systole. Alteration in the abundance and alignment of elastic fibers can result in aortic valve

diseases (Cocciolone et al., 2018). In addition, these elastic fibers bear mechanical load at low strain, enabling the leaflet in the AoV to stretch passively before bearing the load (Vesely, 1997). In vascular tissues, like the aorta, elastin degradation caused by elastases leads to the production of elastin-derived peptides (EDP) (Gayral et al., 2014). These peptides can accelerate the progression of the disease by promoting LDL (low-density Lipoprotein) oxidation and calcification of the vascular wall causing vascular calcification and atherosclerosis (Newby, 2012). Similarly, infiltration of lymphocytes and macrophages into the vessel wall, and the subsequent the destruction of elastin and collagen in the tunica media and adventitia, can result in a loss of smooth muscle cells, thinning of the media, neovascularization, and ultimately formation of aortic aneurysms (Kent, 2014). Though elastic fiber remodeling has been associated with pathological aortic valve remodeling, the exact mechanisms is still unclear in valvular tissues.

In addition, several genetic disorders and mutations can lead to the impairment of ECM in the aortic valve. For instance, supra-valvular aortic stenosis is caused by progressive calcium and scar tissue buildup or congenital defect (bicuspid valve) or Rheumatic Heart disease. Aortic regurgitation is another result of structural abnormality in the ECM of the valve, where the valve loses its elasticity and fails to close correctly. These most common aortic valve diseases are a result of elastin degradation due to aging and various factors (Heinz, 2021).

Elastin has a very slow turnover rate and a half-life of more than 70 years due to its cross-linked nature, which makes it resistant and long-lasting. It is estimated that elastic fibers undergo over 3 billion cycles of extension and recoil during a human lifespan (Duca et al., 2016). The morphology and composition of elastin fibers in the valves and arteries are affected by slow turnover rate, aging mechanical fracture, calcification and proteolytic factor (O'Rourke et al., 2010). The gradual onset of

cardiovascular events is caused by aging due to the gradual fatigue and breakdown of the elastic lamellae in the proximal aorta. In addition, repeated mechanical loading changes the structure of elastin resulting in an increase in tissue calcification which ultimately leads to the rupture of cardiovascular tissues due to an increase in blood pressure and stiffness.

Likewise, mechanical failure in the valve is also due to the repetitive stretching and relaxing of the aortic valve over a lifetime of cardiac cycles, leading to fatigue and eventual rupture of the elastic fibers. With aging there is a reduction in the amount of elastin in the valves making them thicker and less elastic, resulting in increased stiffness. When these valves become stiffer, the aortic valve doesn't close properly causing an increase in the preload and afterload and wall shear stress. The vascular tissues in the left ventricle compensate for this by increasing the wall thickness to maintain the cardiac output. However, this decreases the systolic function of the heart over time, and the valve needs to be replaced to improve cardiac function( (Maganti et al., 2010). This highlights the importance of maintaining the health of elastic fibers in the aorta and aortic valves to prevent cardiovascular events in elderly individuals.

These conditions highlight the far-reaching impact that elastic fiber deficiency, degradation, and valvular failure can have on the body and the importance of understanding the causes and effects of elastic fiber-related diseases for effectively managing and treating these conditions. Currently, treatment options for valve disease caused by elastin degradation and deficiency include surgery for valve replacement or repair (Iung et al., 2003). This study aims to investigate the role of valvular components like Melanocyte, in increasing elastogenesis in heart valves and tissues in the body to improve the treatment options for common elastin-related diseases.

### 1.1.2.3 Melanocytes and Elastin Phenotypes in Mice

Melanocytes are complex cells that have a crucial role in humans' and other animals' skin, hair, and eyes. They provide color to these structures and protect them from harmful ultraviolet radiation. However, melanocytic VICs are also found in mammalian heart tissues yet no studies have been done for the presence of pigment in larger mammals. Melanin pigmentation has been observed in the Aortic valve of commonly used laboratory C57BL/6 (wild type) mice which inhibits the Aortic valve histological study due to these dark pigmentations (Balani et al., 2009) as shown in figure 1.2.2.1. Also, the presence of pigment in the mouse AoV can impact the patterning of elastic fibers and cause increased stiffness in areas with higher pigmentation compared to areas with lower pigmentation (Nasim et al., 2021). Pigmented mice AoV displayed increased elastic fibers and elastin gene expression.

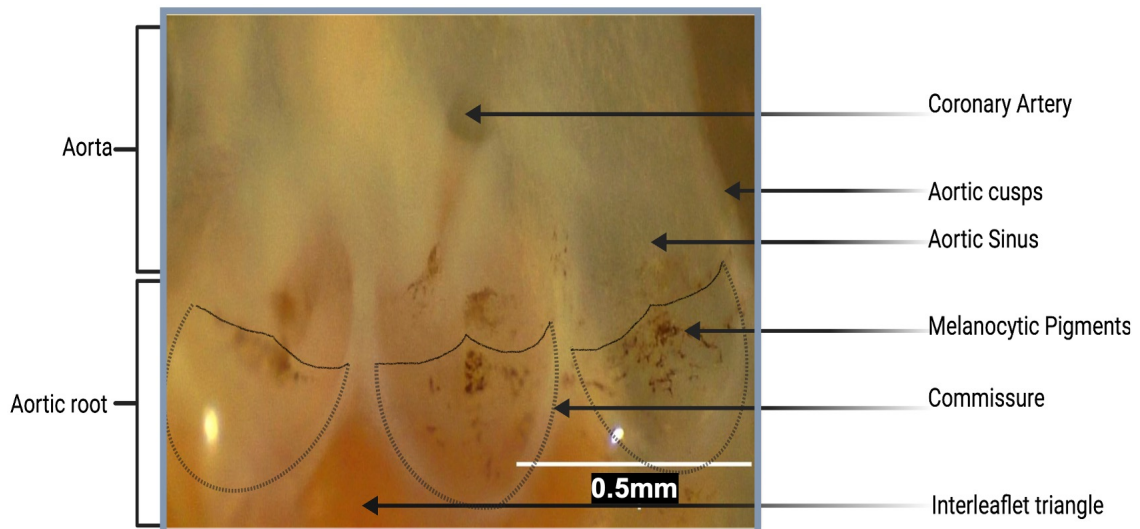


Figure 1.3: Figure showing the pigments in the leaflets of C57BL/6J (WT) mouse .

In contrast, non-pigmented mice AoV showed reduced elastic fibers and elastin gene expression (Hutcheson et al., 2021), implying these overlooked melanocytic cells may have an additional role in the specific demands of the mouse aortic valve biome-

chanics. However, the direct involvement of Melanocytic VICs in generating elastin in the aortic valves of mice is still not clear (Hutcheson et al., 2021). Since these Melanocytic cells play a role in valve stiffness, it is possible that these melanocytic cells might be responsible for generating elastin in mouse aortic valves, this makes them a promising target for therapeutic approaches and tissue engineering aimed at stimulating elastin production in human aortic valves.

### 1.1.3 Research questions

Here, we posed the following questions to better understand the role of melanocytic cells and pigmentation in elastic fiber synthesis in the AoV.

1. Is the elastic fiber abundance affected by differences in melanocytic cells and melanocytic pigment across the three AoV cusps? How do they correlate with each other?
2. Is there any difference in the elastic fiber abundance within the three cusps?

These questions facilitated the development of our experimental protocol, which aims to investigate the correlation between melanocytic pigment, melanocytic cells, and the abundance of elastin within the AoV cusps of mice.

**Specific Aim:** Determine the correlation between elastic fiber abundance, melanocytic expression, and the presence of pigmentation within the AoVs of different mouse models.

## CHAPTER 2

### METHODOLOGY

#### 2.1 Animals used

Animals used: C57BL/6J (Common name: Wild-type mice-WT), B6(Cg)-Tyrc-2J/J mice (Common name: Albino) and KitHet (KH) were used for the study. All mice used were hosted in Animal Care Facility at Florida International University. These WT and Albino mice were bought from Jackson Laboratory for this project. The heterozygous mutant of Kit mice (Kit Heterozygous) were utilized for this study. This heterozygous mutants were obtained by crossing the Kit homozygous with WT (C57BL/6J). The animal protocol was approved by Institutional Animal Care and Use Committee (IACUC). In order to test our hypothesis, we utilized pigmented WT mice along with non-pigmented Albino and KH mice. This selection of mice was chosen as it provides a suitable comparison for evaluating pigmentation within the mouse model.

#### 2.2 Fluorescence Staining/Elastin-Collagen Assay

AF633 (Alexa Flour 633 hydrazide; 1:2000 from Invitrogen, Waltham, MA, Cat# A30634) and CNA35 (1:200, which was a kind gift from Carlijn Bouten) were used for staining the elastic and collagen fibers respectively in the Aortic valve cusps. Previous studies have shown that AF633 binds specifically with elastin fibers without causing tissue autofluorescence (Shen et al., 2012). Also, the CNA35 specifically bonded with collagen fibers as previously studied (Aper et al., 2014). Here we used a 1:200 concentration of CNA35 in PBS (1x) along with a 1:2000 concentration of AF633 (633nm wavelength) to stain our Aortic valve cusps.

### 2.2.1 Procedure

Alexa Flour 633 (AF633) and CNA35 were used for staining the elastin-based elastic fibres and collagen fibers respectively in the AoV cusps. Previous studies have shown that AF633 binds specifically with elastin fibers without causing tissue autofluorescence (Shen et al., 2012). CNA35 specifically binds to collagen fibers as previously studied by (Aper et al., 2014). Here, we used a 1:200 concentration of CNA35 in PBS (1x) along with a 1:2000 concentration of AF633 (633nm wavelength) in order to stain the AoV cusps.

WT, Albino and KH mice were euthanized using CO<sub>2</sub> gas and spinal dislocation was done prior to dissection. The hearts were extracted and kept in 1x PBS on ice. The hearts were transported on ice for AoV dissection. Images of the freshly dissected AoVs were taken under a conventional light microscope to obtain bright-field images. Subsequently, the extracted AoVs were treated with 4% Paraformaldehyde (PFA-Thermo Scientific), washed with 1xPBS and fixed at room temperature for 15-20 minutes, and in overnight for bleaching in 10% hydrogen peroxide (H<sub>2</sub>O<sub>2</sub>)(Fisher Scientific H325-100) mixed with PBS to remove visible pigments. The bleached tissues were washed and prepared for whole-mount staining.

All three cusps from each valve were extracted, placed on a slide, and then stained for elastin and collagen with Alexa Flour 633 and CNA35 mix. The slide was kept at room temperature for 15-20 minutes to allow proper staining of the fibers. The tissue mounted slides were then washed five times before finally being covered with a thin cover slip using mounting media (Fluoromount-G Mounting Medium, Invitrogen Thermofisher).

### 2.2.2 Imaging

For imaging, an inverted Confocal Microscope Nikon C1 with a 20x objective was used to generate z-stack optical section images of the tissue. The 3D structure of each leaflet was reconstructed, and further analyses was performed using Matlab and NIH ImageJ Fiji.

### 2.2.3 Image Quantification

To quantify fluorescence in the stained tissue, the images opened in NIH ImageJ Fiji. These large .nd2 files obtained from Confocal were converted into .tif files using ImageJ. We built a customized Matlab script for further image quantification. Our Matlab script was designed to generate a Maximum Intensity Projection (MIP) of elastin and collagen fluorescent images. Here we assigned a consistent threshold in all images in order to remove the noise in the elastin-collagen fluorescence images and find the intensity of elastin fluorescence. This measured elastin fluorescence intensity was averaged to get the Mean fluorescence intensity for each aortic cusp. The thresholds were kept constant for all the samples.

Similarly, another threshold was simultaneously adjusted for each image for area calculation. The MIP images for each elastin and collagen assay were binarized and added together in order to find the area of each cusp surface individually (fig. B, E, H). Our code made sure that none of the pixels were repeated when adding these two areas. The mean fluorescence intensities of elastin obtained using the earlier threshold were normalized with the surface area of each cusp, (fig. C, F, I) and the data was visualized using Graph-Pad Prism. To statistically analyze the obtained data, a one-way ANOVA test was performed to compare the data from these two types of mice. This allowed for an accurate comparison of the mean fluorescence

intensities between the different samples and helped to determine any significant differences.

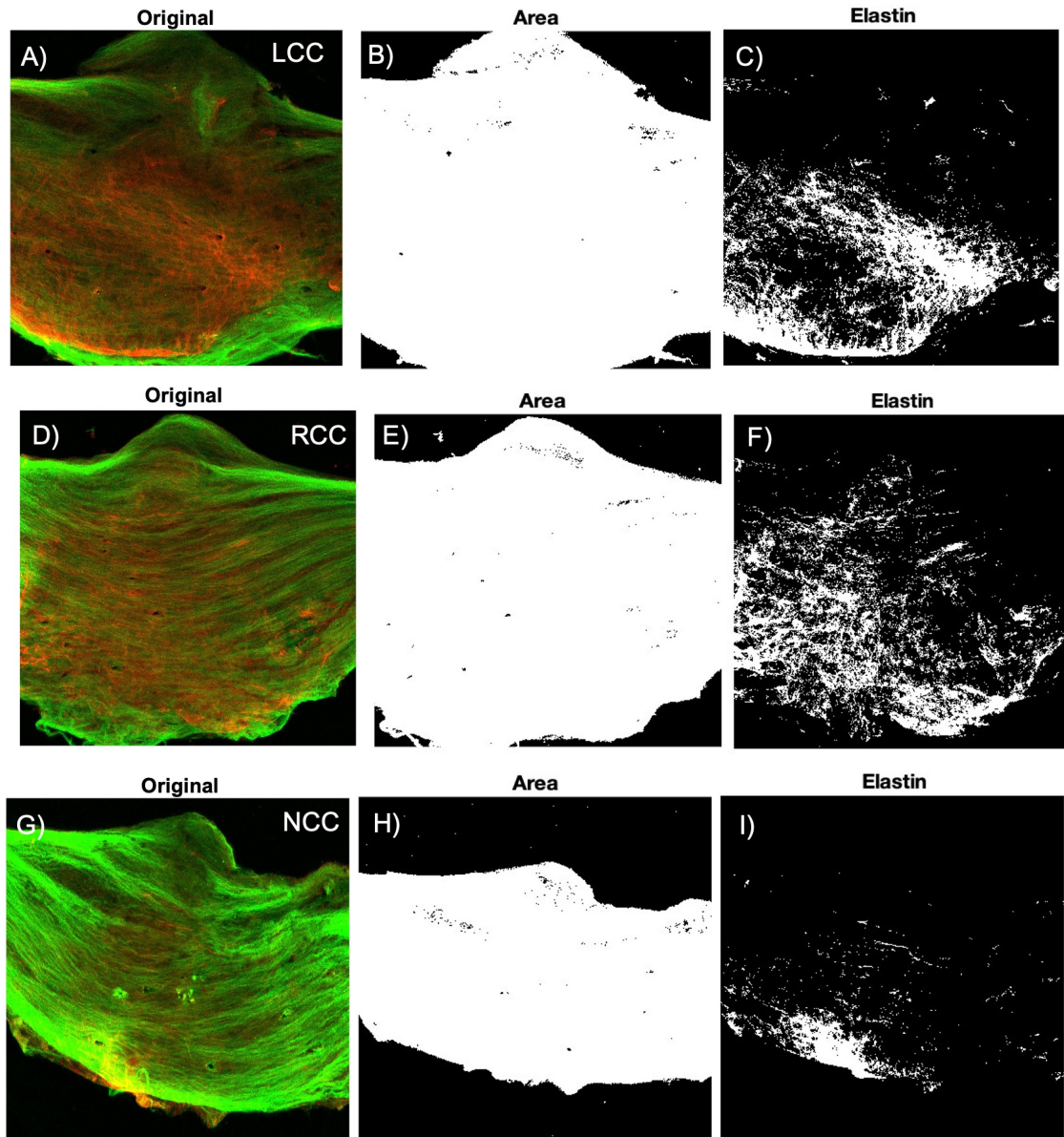


Figure 2.1: The figure illustrates the elastic(in red) and collagen(in green) fibers present in the leaflets of the AoV. Customized code and threshold are utilized to determine the area of each leaflet (Fig. B, E, H). Additionally, the MFI of AF633 is employed to measure the elastin abundance within the leaflets (Fig. C, F, I).

## 2.3 RT-qPCR Reverse Transcription quantitative Polymerase

### Chain reaction

For the transcriptomic analysis of the melanocytic marker, we added all the three cusps of aortic valve from each biological replicate in 750 $\mu$ l of Trizol(Thermo Fisher Scientific 15596026) and keep it at -80°C until RNA extraction. The RNA from each biological replicates sample was extracted following the Invitrogen RNA extraction (Trizol Reagent method) from Thermofisher Scientific. The RNA yield was quantified using the Nanodrop Spectrometer(Thermo Scientific) in the BME Core facility laboratory at FIU.

For cDNA extraction, 9 $\mu$ l of extracted RNA from each biological replicate was added to 2X reverse transcription master mix as per Thermofisher scientific protocol. The thermal cycle was be programmed to 25°C for 10 minutes, 37°C for 120 minutes, 85°C for 5 minutes and 4°C for infinite time respectively. Next, RT-qPCR was performed using a commercially available Powerup SYBR Green Master Mix based on the protocol from Applied Biosystem. Dopachrome Tautomerase (DCT) and Tyrosinase (Tyr) was be used as primers for the melanocytic marker (Hulin et al, 2019). GAPDH was used as the house keeping gene. The primer sequences were as given in table 2.2.

Two replicates of each were created using 9  $\mu$ l of master mix with 1 $\mu$ l of cDNA in 48 well plate PCR setting. The PCR machine was set as 50°C for 2 minutes and 95°C for 2 minutes for holding; 95°C for 15s, 55°C for 15s and 72 for 1 minute for cycling and 95°C for 15, 60°C for 1minute and 95°C for 15 seconds again for 40 cycles. The melt curve was then generated, and the baseline and threshold cycle (CT) were calculated based on the obtained results. The  $\delta$ Ct was calculated by normalizing the CT value with the obtained GAPDH value. The relative melanocytic expressions

Primer	Sequence	
DCT	FW	CCT GTC TCT CCA GAA GTT TGA C
	RV	CCA GTG TTC CGT CTG CTT TA
TYR	FW	CAC TGG TGG GAG CTG TTA TT
	RV	GCT GTG GTA GTC GTC TTT GT
GAPDH	FW	AAC AGC AAC TCC CAC TCT TC
	RV	CCT GTT GCT GTA GCC GTA TT

Figure 2.2: Table 1: Primer DCT, TYR, GAPDH along with their sequences.

were expressed using the  $2^{-\delta\delta C_t}$  method.

## CHAPTER 3

### RESULTS

**Specific Aim:** To determine the correlation between elastin abundance, expression of melanocytic markers, and the presence of pigmentation within the AoV of different mouse models.

#### **3.1 Pigmentation in WT1, WT2, Albino, KH:**

To study the pigmentation pattern in different mouse models, extracted AoV leaflets were divided into four separate groups based on their pigmentation level (fig 3.1). We observed noticeable differences in pigmentation levels between the mouse models, with WT mice exhibiting full to partial pigmentation (fig. 3.1A, 3.1B), whereas Albino and KH mice had no pigmentation (fig.3.1C, 3.1D). Among the WT mice, all three leaflets (left, right and non-coronary) were pigmented about 56% of the time (WT1, n=43), whereas the left coronary leaflets lacked pigmentation approximately 44% of the time (WT2, n=43). Pigmentation was most prominent in the belly region of the leaflets in the WT mice (fig. 3.1A, 3.1B).

#### **3.2 Elastin Abundance in WT1, WT2, Albino and KH:**

To study the abundance of elastic fibers in these mouse models, we quantified the fluorescent signal obtained from leaflets stained with AF633(for elastin) and CNA35(for Collagen). Similar to previous observations in AoV of larger mammals, elastic fibers were radially aligned within the ventricularis layer of the leaflets and becomes circumferentially aligned towards the fibrosa layer of the leaflets (fig. 3.2A, 3.2B). We observed distinct trilaminar layers within the AoV leaflet despite the microscopic size

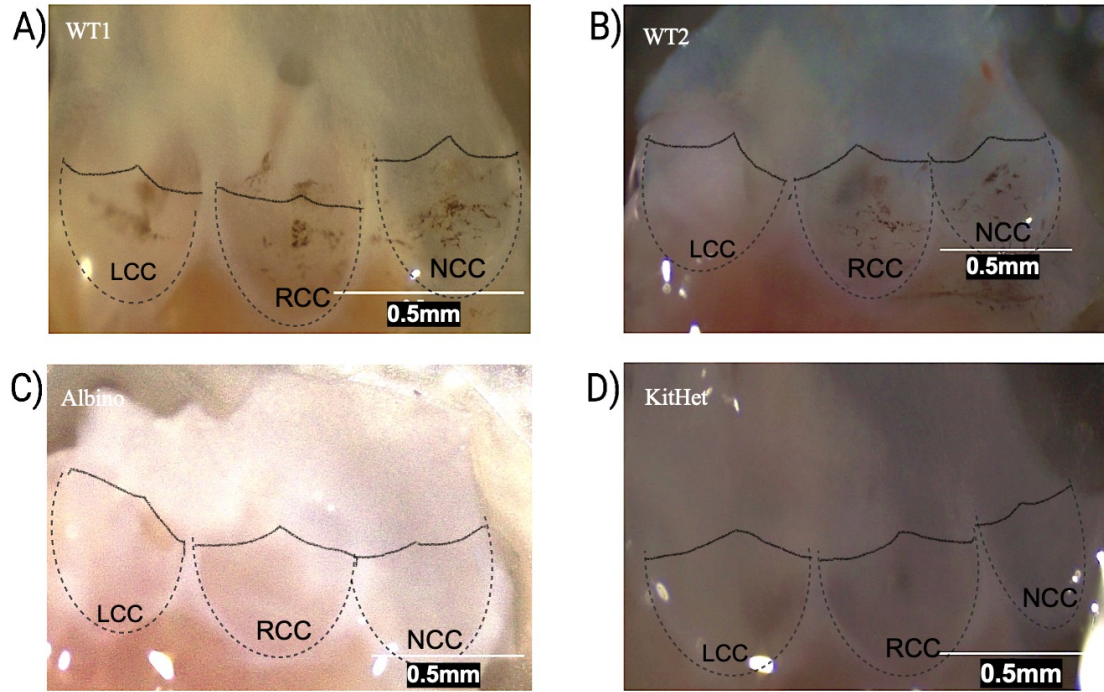


Figure 3.1: The aortic valve structure showing the melanocytic pigments and different section in the valve apparatus. In 56% of WT mice, all LCC, RCC and NCC are pigmented. B) In 44% of the WT mice, the LCC doesn't have melanocytic pigments whereas the RCC and NCC are pigmented. C) and D) The Albino and the KitHet mice (respectively) doesn't have pigment in any of the cusps.

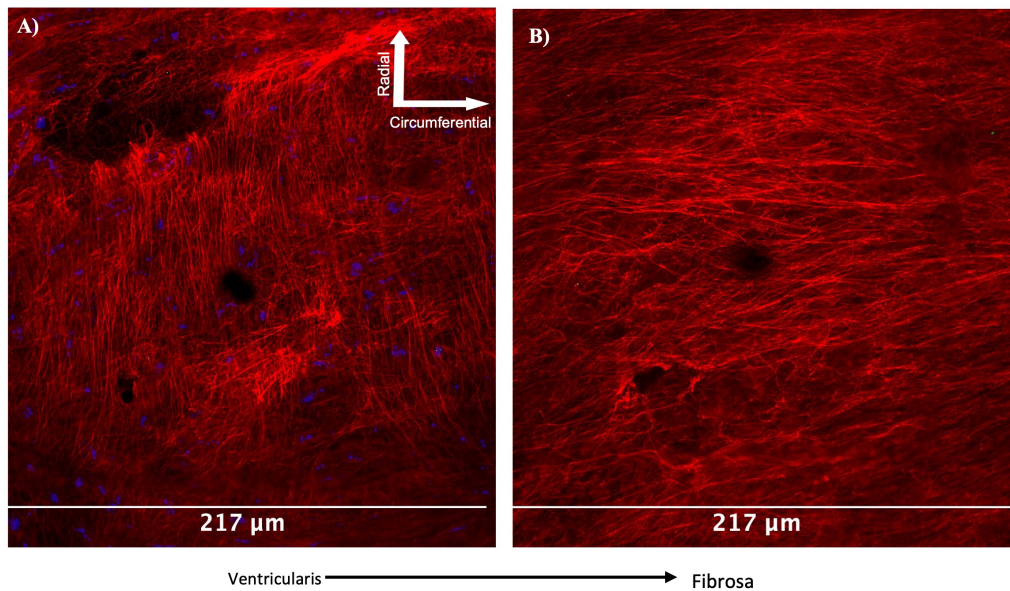


Figure 3.2: Elastin based elastic fibre alignment in AoV leaflets-In murine AoV leaflets, these elastic fibers on the ventricularis surface of the valve cusp are aligned radially A), and they transition to a circumferential orientation as they approach the fibrosa B)

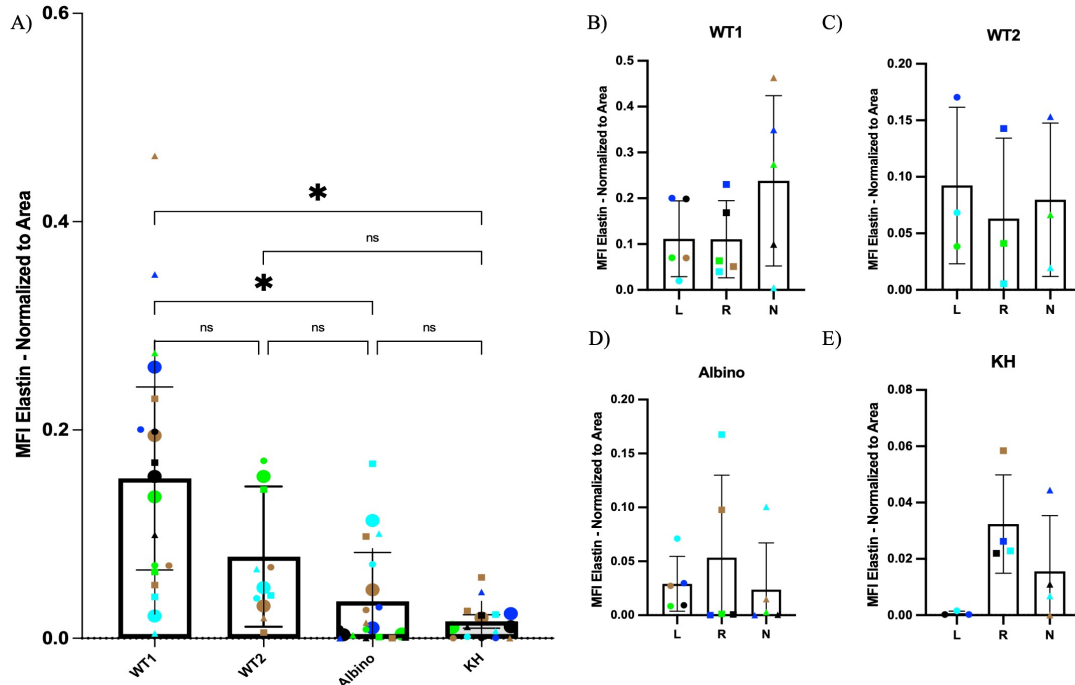


Figure 3.3: Elastic fibers abundance in the AoV leaflets in different mouse models. Fig 3.3A shows the fiber abundance in WT1, WT2, Albino and KH mice normalized to the area of the respective leaflets. Fig 3.3B,3.3C, 3.3D, 3.3E shows the varying amount of elastic fiber in LCC, RCC, NCC of AoV leaflets in these classified four groups, WT1, WT2, Albino, and KH respectively.)

of the leaflet. The ventricularis tends to exhibit more elastin fibers than the other regions within the leaflets. To quantify the elastic fiber abundance in each leaflet, the mean fluorescence intensity of each leaflet was calculated using a customized MATLAB script and subsequently normalized by total area, as discussed above(fig.2.1). We observed significantly higher elastic fiber abundance in the WT1(n=5) leaflets compared to albino (n=5) and KH(n=4) leaflets with p-values =0.0357 and 0.0235 respectively, as shown in fig. 3.3A. We observed no significant difference in elastic fiber abundance between the partially pigmented WT2(n=3), Albino(n=5) and KH(n=4) mouse models (fig. 3.2A). We did not observe any statistically significant differences in elastic fiber abundance between the three leaflets in any of the mouse populations studied (fig. 3.3B, 3.3C, 3.3D, 3.3E)

### 3.3 Melanocytic expression in WT1, WT2, Albino and KH:

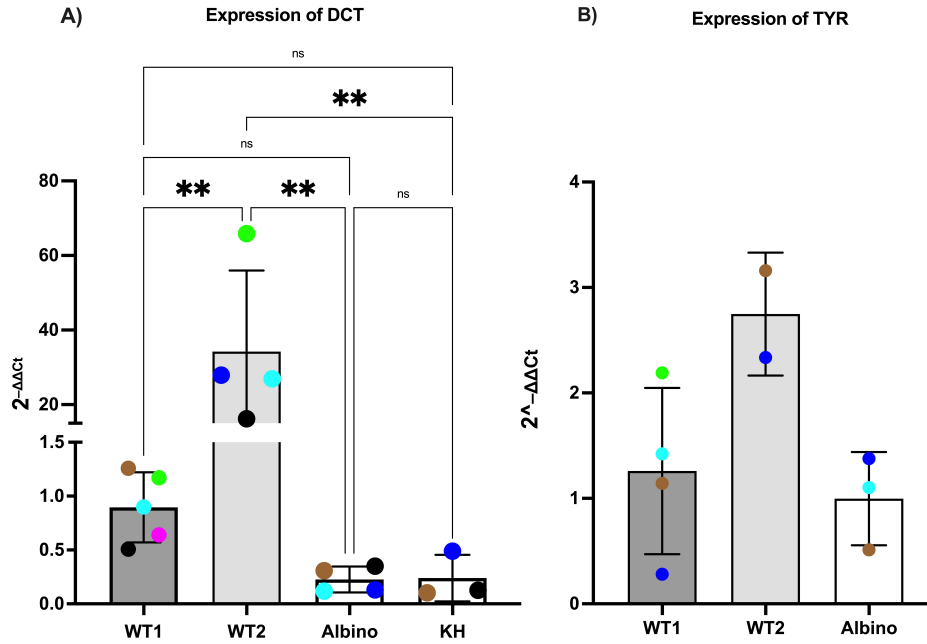


Figure 3.4: Expression of DCT within the AoV leaflets in different mouse models showing significant difference between the WT2 and the rest of mouse models. However, it does not show any significant difference between the WT1, Albino and KH.

To determine the correlation between the melanocyte presence, pigment production, and elastin abundance we assessed transcriptomic level expression of canonical melanocytic phenotypic markers DCT and Tyrosinase using RT-qPCR. The  $\delta\delta CT$  value was calculated based on the CT value of GAPDH with using WT1 as the control group for comparisons. The WT2 (n=4) leaflets exhibited significantly higher DCT expression compared to the WT1 (n=5), Albino (n=4) and KH (n=3) leaflets (p-values= 0.0031, 0.0040 and 0.0071, respectively) (fig. 3.4). Although the expression of tyrosinase in WT2 trended higher compared to WT1 and Albino, we did not observe any significant differences in Tyr expression between the groups (fig. 3.4). The KH mice (n=3) did not exhibit Tyr expression. These individual differences may be due potential genetic differences between individual mice.

## CHAPTER 4

### DISCUSSION

In murine AoV, the elastic fibers are more radially aligned in the ventricularis and becomes circumferentially aligned towards the fibrosa layer of the leaflets. Previous studies have reported diminished elastic fibers and elastin expression in hypopigmented mice whereas hyperpigmented mice had disorganized fiber patterning and expressed more elastin (Nasim et al, 2021; Hutcheson et al, 2021). However, the exact connection between the presence of pigmentation, melanocytic marker expression, and elastic fiber abundance in elastogenesis hasn't been established. This research aimed to establish a correlation between these three components in the AoV.

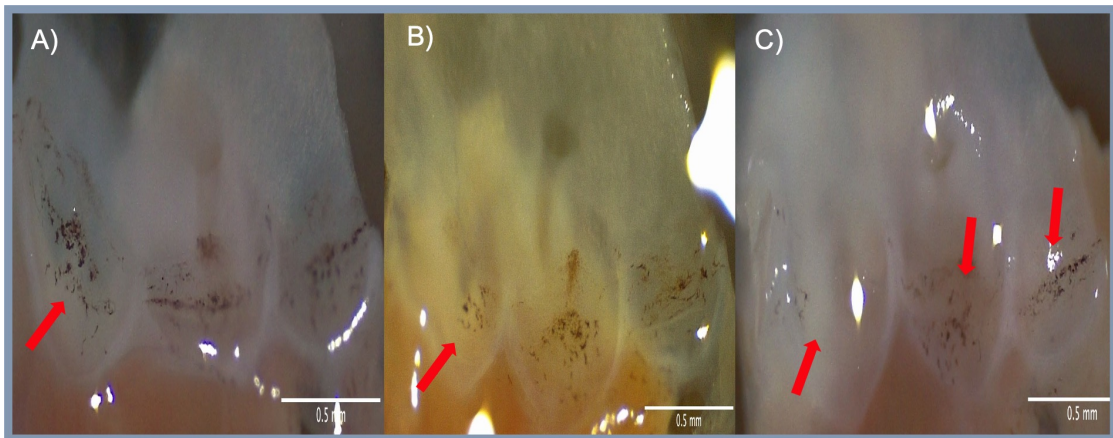


Figure 4.1: Different levels of pigmentation seen in the leaflets. The LCC of (A) has more pigments than the LCC in fig. (C) (shown by red arrow). The cause of this different level of pigmentation is still unclear and requires more detailed cellular study.

To accomplish this, we utilized three types of mice: WT mice with pigmentation on the skin and AoV leaflets; albino mice, which are not able to produce pigmentation due to a mutation in the tyrosinase gene (Jackson and Bennett, 1990); and KH mice, which exhibit pigmentation on the skin but not in the AoV leaflets due to melanocytic dysfunction. The observed dysfunction in pigment synthesis may be

attributed to reduced kit ligand levels resulting from neural crest migration, which ultimately affects the cells ability to produce pigments in the AoV. In addition, we also noticed differences in the pigmentation patterning in the AoV leaflets of the WT mice, wherein some mice exhibited pigmentation across all three leaflets, and some were devoid of pigmentation in the left coronary leaflet. Interestingly, among the pigmented leaflets, there exists a variation in the levels of pigmentation, with some leaflets exhibiting abundant pigmentation while others have lower levels (4.1). The underlying cause for this variation is not clear.

Furthermore, in the quantitative assessment of elastic fiber abundance in the AoV leaflets among the groups mentioned earlier, we observed the pigmented WT1 mice exhibited statistically higher abundance of elastic fibers compared to the non-pigmented Albino and KH mice. However, the difference in elastic fiber abundance between the WT1 group and the partially pigmented WT2 group was not statically significant. Although, we observed trending differences in elastic fiber abundance within the leaflets in each mouse model, the differences did not reach statistical significance. Our findings suggest that, while genetic deficiencies in pigment production lead to elastin phenotypes, the presence of pigmentation alone does not predict the abundance of elastic fibers in WT AoV leaflets.

Despite previous reports on the pigmentation in murine AoV leaflets and elastin expression, the association between expression of melanocytic markers and elastic fiber abundance remains unclear. In this study, we assessed the expression of the melanocytic markers DCT and TYR. This data revealed higher expression of both DCT(n=4) and TYR(n=2) genes in the AoV leaflets of partially pigmented WT2 mouse compared to the fully pigmented WT1 and non-pigmented Albino and KH groups. Our data indicate that the relative abundance of melanocytes alone is not sufficient to explain the previously observed elastin phenotypes, as we did not

observe a significant difference in the abundance of elastic fibers between WT2 and the other studied groups (WT1, Albino, and KH). Our results suggest additional mechanisms contribute to elastogenesis beyond pigmentation or melanocytic gene expression. However, it should be noted that our sample size was small. Ongoing analyses will increase the sample size to increase the statistical power of our analysis.

The AoV is a heterogeneous structure consisting of endothelial, interstitial, immune, glial, and melanocytic cells. Even within the population known as “VICs,” there are different subpopulations that produce specific types of ECM during the development of the valve layers (Liu et al., 2007). The developmental origin and contributions to adult-onset remodeling for each of these lineages are not fully understood. Previous studies have shown the involvement of  $\alpha$ SMA-positive fibroblasts in elastogenesis in other tissues (Liu et al., 2014). However, whether  $\alpha$ SMA-positive cells play a similar role in the AoV and interactions with cells expressing phenotypic markers of neurons, immune cells, and glial cells has not been established. Additionally, fetal AoVs exhibit higher expression of fibroblastic markers FBN2 and FBN3 in the ventricularis, which decrease with age along with the decrease in elastin expression (Carta et al., 2006; Votteler et al., 2013), potentially supporting a role for fibroblast in cells in AoV elastin patterning during development. Lineage tracing studies are needed to better understand the developmental derivation of AoV cellular phenotypes and their role in patterning of elastin and other extracellular matrix components.

Elastin protein is primarily synthesized and accumulates during the fetal and neonatal stages of development. Given the long half-life of elastin, very little is produced after the mature AoV forms (Kelleher et al., 2004). However, the quantity of elastin gradually declines with age owing to slow turnover. The expression of DCT decreases, the melanin production increases, and elastin expression de-

creases from P7 to P30 during the postnatal development of the heart valves in mice (Hulin et al., 2019). These findings highlight the dynamic changes in the expression of melanocytic traits and elastogenesis during heart valve development. However, it should also be noted that melanin pigment has not been observed in human (AoV), despite the presence of melanocytic markers (DCT and TRP1) in the human AoV (Hutcheson et al., 2021). Interestingly, the distribution of these markers in the human AoV closely mirrors their localization in murine leaflets ((Hutcheson et al., 2021). It is possible that melanocytic cells perform a similar function in AoV extracellular matrix patterning but do not produce pigment in the human AoV or that pigment is lost during the developmental process.

Elastin expression is first observed in the fetus at 4 weeks of development as the blood flow and pressure exhibit sharp increases (Faury, 2001; Riem Vis et al., 2011), suggesting that bio-mechanical factors likely play an important role in elastogenesis. A comprehensive study on the aortic valve development can provide better insights into the process of elastogenesis.

## CHAPTER 5

### CONCLUSION

Despite the differences in elastic fiber abundance due to the genetic alterations in melanocytic populations, our data demonstrate that neither the presence/absence of melanocytic markers nor abundance of pigmentation is sufficient to explain the elastin phenotype. Further studies are needed to understand the role of melanocytic populations in elastogenesis during AoV development. In addition to assessing expression of elastin directly, future studies should also assess potential melanocytic contributions to other constituents involved in elastic fiber formation such as elastin binding protein, microfibril-associated glycoprotein-1, and desmosine, an amino acid unique to elastic fibers (Thomas et al, 1963).

Elastic fiber degradation induces valvular and vascular calcification (Aikawa et al, 2009). For several decades, researchers in the space of regenerative medicine have attempted to replicate the complex structure and mechanics of a native AoV either in situ or through tissue engineered constructs, but consistent regeneration/production of elastic fibers has proven challenging. A thorough understanding of the developmental changes in the AoV and their relationship to elastogenesis may help to elucidate the pathogenesis of aortic valve disorders and pave a way for new diagnostic and therapeutic strategies.

## REFERENCES

- [1] Balani, K., Brito, F. C., Kos, L., Agarwal, A. (2009). Melanocyte pigmentation stiffens murine cardiac tricuspid valve cusp. *J R Soc Interface*, 6(40), 1097-1102. <https://doi.org/10.1098/rsif.2009.0174>
- [2] Bischoff, J., Aikawa, E. (2011). Progenitor cells confer plasticity to cardiac valve endothelium. *J Cardiovasc Transl Res*, 4(6), 710-719. <https://doi.org/10.1007/s12265-011-9312-0>
- [3] Carneiro, F., Kruithof, B. P., Balani, K., Agarwal, A., Gaussin, V., Kos, L. (2015). Relationships Between Melanocytes, Mechanical Properties and Extracellular Matrix Composition in Mouse Heart Valves. 25(1-2), 17-26. <https://doi.org/10.1615/JLongTermEffMedImplants.2015011748>
- [4] Carruthers, C. A., Alfieri, C. M., Joyce, E. M., Watkins, S. C., Yutzey, K. E., Sacks, M. S. (2012). Gene expression and collagen fiber micromechanical interactions of the semilunar heart valve interstitial cell. *Cellular and molecular bioengineering*, 5, 254-265.
- [5] Hutcheson, J. D., Schlotter, F., Creager, M. D., Li, X., Pham, T., Vyas, P., Higashi, H., Body, S. C., Aikawa, M., Singh, S. A., Kos, L., Aikawa, E. (2021). Elastogenesis Correlates With Pigment Production in Murine Aortic Valve Cusps [Original Research]. *Frontiers in Cardiovascular Medicine*, 8. <https://doi.org/10.3389/fcvm.2021.678401>
- [6] Karnik, S. K., Brooke, B. S., Bayes-Genis, A., Sorensen, L., Wythe, J. D., Schwartz, R. S., Keating, M. T., Li, D. Y. (2003). A critical role for elastin signaling in vascular morphogenesis and disease. *Development*, 130(2), 411-423. <https://doi.org/10.1242/dev.00223>
- [7] Mitts, T. F., Bunda, S., Wang, Y., Hinek, A. (2010). Aldosterone and Mineralocorticoid Receptor Antagonists Modulate Elastin and Collagen Deposition in Human Skin. *Journal of Investigative Dermatology*, 130(10), 2396-2406. <https://doi.org/https://doi.org/10.1038/jid.2010.155>
- [8] Nasim, S., Pandey, P., Kanashiro-Takeuchi, R. M., He, J., Hutcheson, J. D., & Kos, L. (2021). Pigmentation Affects Elastic Fiber Patterning and Biomechanical Behavior of the Murine Aortic Valve [Original Research]. *Frontiers in Cardiovascular Medicine*, 8. <https://doi.org/10.3389/fcvm.2021.754560>

- [9] Rajamannan, N. M., Evans, F. J., Aikawa, E., Grande-Allen, K. J., Demer, L. L., Heistad, D. D., Simmons, C. A., Masters, K. S., Mathieu, P., O'Brien, K. D., Schoen, F. J., Towler, D. A., Yoganathan, A. P., & Otto, C. M. (2011). Calcific aortic valve disease: not simply a degenerative process: A review and agenda for research from the National Heart and Lung and Blood Institute Aortic Stenosis Working Group. Executive summary: Calcific aortic valve disease-2011 update. *Circulation*, 124(16), 1783-1791. <https://doi.org/10.1161/circulationaha.110.006767>
- [10] Saitow, C., Kaplan, D. L., & Castellot, J. J. (2011). Heparin stimulates elastogenesis: application to silk-based vascular grafts. *Matrix Biology: Journal of the International Society for Matrix Biology*, 30(5-6), 346-355. <https://doi.org/10.1016/j.matbio.2011.04.005>
- [11] Sherratt, M. J. (2009). Tissue elasticity and the aging elastic fiber. *Age (Dordr)*, 31(4), 305-325. <https://doi.org/10.1007/s11357-009-9103-6>
- [12] Aggoun, Y., Sidi, D., Levy, B., Lyonnet, S., Kachaner, J., Bonnet, D. (2000). Mechanical properties of the common carotid artery in Williams syndrome. *Heart*, 84(3), 290-293.
- [13] Billiar , K. L., & Sacks , M. S. (1999). Biaxial Mechanical Properties of the Natural and Glutaraldehyde Treated Aortic Valve Cusp—Part I: Experimental Results. *Journal of Biomechanical Engineering*, 122(1), 23-30. <https://doi.org/10.1115/1.429624>
- [14] Cocciolone, A. J., Hawes, J. Z., Staiculescu, M. C., Johnson, E. O., Murshed, M., Wagenseil, J. E. (2018). Elastin, arterial mechanics, and cardiovascular disease. *Am J Physiol Heart Circ Physiol*, 315(2), H189-h205. <https://doi.org/10.1152/ajpheart.00087.2018>
- [15] Duca, L., Blaise, S., Romier, B., Laffargue, M., Gayral, S., El Btaouri, H., Kawecki, C., Guillot, A., Martiny, L., Debelle, L., & Maurice, P. (2016). Matrix ageing and vascular impacts: focus on elastin fragmentation. *Cardiovascular Research*, 110(3), 298-308. <https://doi.org/10.1093/cvr/cvw061>
- [16] Gayral, S., Garnotel, R., Castaing-Berthou, A., Blaise, S., Fougerat, A., Berge, E., Montheil, A., Malet, N., Wymann, M. P., Maurice, P. (2014). Elastin-derived peptides potentiate atherosclerosis through the immune Neu1-PI3K pathway. *Cardiovascular Research*, 102(1), 118-127. <https://doi.org/10.1093/cvr/cvu016>

- [17] Heinz, A. (2021). Elastic fibers during aging and disease. *Ageing Res Rev*, 66, 101255. <https://doi.org/10.1016/j.arr.2021.101255>
- [18] Iung, B., Baron, G., Butchart, E. G., Delahaye, F., Gohlke-Bärwolf, C., Levang, O. W., Tornos, P., Vanoverschelde, J.-L., Vermeer, F., Boersma, E., Ravaut, P., & Vahanian, A. (2003). A prospective survey of patients with valvular heart disease in Europe: The Euro Heart Survey on Valvular Heart Disease. *European Heart Journal*, 24(13), 1231-1243. [https://doi.org/10.1016/s0195-668x\(03\)00201-x](https://doi.org/10.1016/s0195-668x(03)00201-x)
- [19] Kent, K. C. (2014). Abdominal aortic aneurysms. *New England Journal of Medicine*, 371(22), 2101-2108. <https://doi.org/10.1056/nejmcp1401430>
- [20] Ku, C.-H., Johnson, P. H., Batten, P., Sarathchandra, P., Chambers, R. C., Taylor, P. M., Yacoub, M. H., Chester, A. H. (2006). Collagen synthesis by mesenchymal stem cells and aortic valve interstitial cells in response to mechanical stretch. *Cardiovascular Research*, 71(3), 548-556. <https://doi.org/10.1016/j.cardiores.2006.03.022>
- [21] Latif, N., Sarathchandra, P., Taylor, P. M., Antoniow, J., Yacoub, M. H. (2005). Localization and pattern of expression of extracellular matrix components in human heart valves. *J Heart Valve Dis*, 14(2), 218-227.
- [22] Lincoln, J., & Yutzey, K. E. (2011). Molecular and developmental mechanisms of congenital heart valve disease. *Birth Defects Research Part A: Clinical and Molecular Teratology*, 91(6), 526-534. <https://doi.org/https://doi.org/10.1002/bdra.20799>
- [23] Newby, A. C. (2012). Matrix metalloproteinase inhibition therapy for vascular diseases. *Vascular pharmacology*, 56(5-6), 232-244.
- [24] O'Rourke, M. F., Safar, M. E., Dzau, V. (2010). The Cardiovascular Continuum extended: aging effects on the aorta and microvasculature. *Vascular Medicine*, 15(6), 461-468.
- [25] Vesely, I. (1997). The role of elastin in aortic valve mechanics. *Journal of Biomechanics*, 31(2), 115-123. [https://doi.org/https://doi.org/10.1016/S0021-9290\(97\)00122-X](https://doi.org/https://doi.org/10.1016/S0021-9290(97)00122-X)
- [26] Mjaatvedt, C. H., Kern, C. B., Norris, R. A., Fairey, S., Cave, C. L. (2005). Normal distribution of melanocytes in the mouse heart. *The Anatomical Record Part A: Discoveries in Molecular, Cellular, and Evolutionary Biology*, 285A(2), 748-757. <https://doi.org/https://doi.org/10.1002/ar.a.20210>

- [27] Green, E. M., Mansfield, J. C., Bell, J. S., & Winlove, C. P. (2014). The structure and micromechanics of elastic tissue. *Interface Focus*, 4(2), 20130058. <https://doi.org/doi:10.1098/rsfs.2013.0058>
- [28] Maganti, K., Rigolin, V. H., Sarano, M. E., Bonow, R. O. (2010). Valvular heart disease: diagnosis and management. *Mayo Clin Proc*, 85(5), 483-500. <https://doi.org/10.4065/mcp.2009.0706>
- [29] Francis, G., John, R., & Thomas, J. (1973). Biosynthetic pathway of desmosines in elastin. *The Biochemical journal*, 136(1), 45-55. <https://doi.org/10.1042/bj1360045>
- [30] Aikawa, E., Aikawa, M., Libby, P., Figueiredo, J.-L., Rusanescu, G., Iwamoto, Y., . . . Weissleder, R. (2009). Arterial and Aortic Valve Calcification Abolished by Elastolytic Cathepsin S Deficiency in Chronic Renal Disease. *Circulation*, 119(13), 1785-1794. [https://doi.org/10.1161/CIRCULATION\\_AHA.108.827972](https://doi.org/10.1161/CIRCULATION_AHA.108.827972)
- [31] Aper, S. J. A., van Spreeuwel, A. C. C., van Turnhout, M. C., van der Linden, A. J., Pieters, P. A., van der Zon, N. L. L., de la Rambelje, S. L., Bouten, C. V. C., & Merckx, M. (2014). Colorful Protein-Based Fluorescent Probes for Collagen Imaging. *PLOS ONE*, 9(12), e114983. <https://doi.org/10.1371/journal.pone.0114983>
- [32] Shen, Z., Lu, Z., Chhatbar, P. Y., O'Herron, P., & Kara, P. (2012). An artery-specific fluorescent dye for studying neurovascular coupling. *Nature Methods*, 9(3), 273-276. <https://doi.org/10.1038/nmeth.1857>
- [33] Alexia Hulin, Luis Hortells, M. Victoria Gomez-Stallons, Anna O'Donnell, Kashish Chetal, Mike Adam, Patrizio Lancellotti, Cecile Oury, S. Steven Potter, Nathan Salomonis, Katherine E. Yutzey, Allon Klein, Barbara Treutlein; Maturation of heart valve cell populations during postnatal remodeling. *Development* 15 June 2019; 146 (12): dev173047. doi: <https://doi.org/10.1242/dev.173047>
- [34] Frank, M. (2006). Fibrillins 1 and 2 Perform Partially Overlapping Functions during Aortic Development *Journal of Biological Chemistry*, 281(12), 8016-8023. <https://doi.org/10.1074/jbc.M511599200>
- [35] Faury, G. (2001). Function-structure relationship of elastic arteries in evolution: from microfibrils to elastin and elastic fibres. *Pathologie Biologie*, 49(4), 310-325. [https://doi.org/https://doi.org/10.1016/S0369-8114\(01\)00147-X](https://doi.org/https://doi.org/10.1016/S0369-8114(01)00147-X)

- [36] Jackson, I. J., & Bennett, D. C. (1990). Identification of the albino mutation of mouse tyrosinase by analysis of an in vitro revertant. *Proc Natl Acad Sci U S A*, 87(18), 7010-7014. <https://doi.org/10.1073/pnas.87.18.7010>
- [37] Kelleher, C. M., McLean, S. E., & Mecham, R. P. (2004). Vascular Extracellular Matrix and Aortic Development. In *Current Topics in Developmental Biology* (Vol. 62, pp. 153-188). Academic Press. <https://doi.org/https>
- [38] Shen, Z., Lu, Z., Chhatbar, P. Y., O'Herron, P., & Kara, P. (2012). An artery-specific fluorescent dye for studying neurovascular coupling. *Nature Methods*, 9(3), 273-276. <https://doi.org/10.1038/nmeth.1857>